An evaluation of the effects of heat ray retro-reflective film on the outdoor thermal environment using a radiant analysis method

Shinji Yoshida (University of Fukui)

Saori Yumino (Tohoku University)

Akashi Mochida (Tohoku University)

Taiki Uchida (Tohoku University)

Table of Contents

1.Background and purpose

2. Outline of revised method for
   radiant computation

3. Outline of analysis

4. Results and discussion

5. Conclusion

Background of this study

- Low-e double glazing and heat-shading films for windows ...

⇨ has been adopted to reduce building cooling loads in the summer.

(However, ...)

⇨ usually reflect solar radiation towards pedestrian spaces.

⇩

Negative effects on thermal comfort of pedestrians!

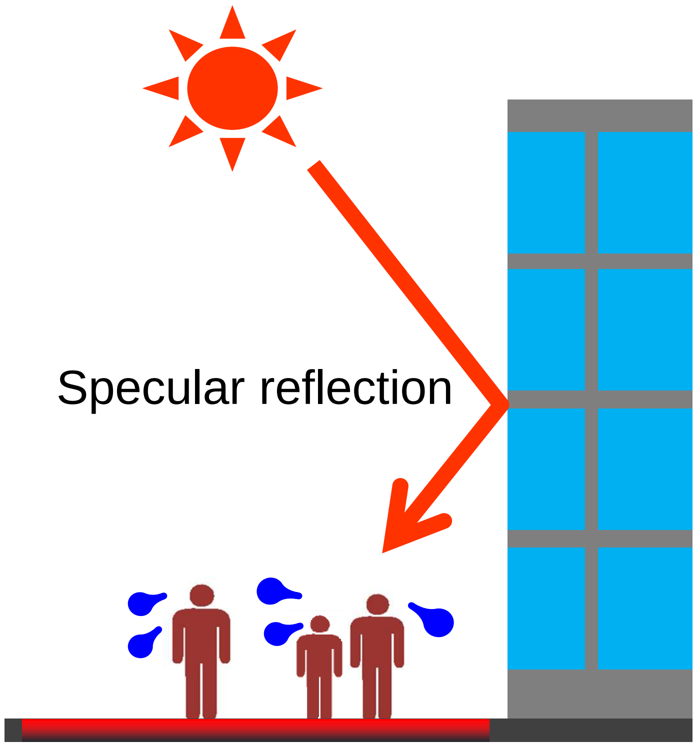

Background this study (2)

- Application of heat ray retro-reflective film to windows enables us to …

  ⇨ return the reflected radiation to the sky.

  ⇩

  reduce the indoor cooling load while mitigating effects on the thermal environment in outdoor spaces near the ground.

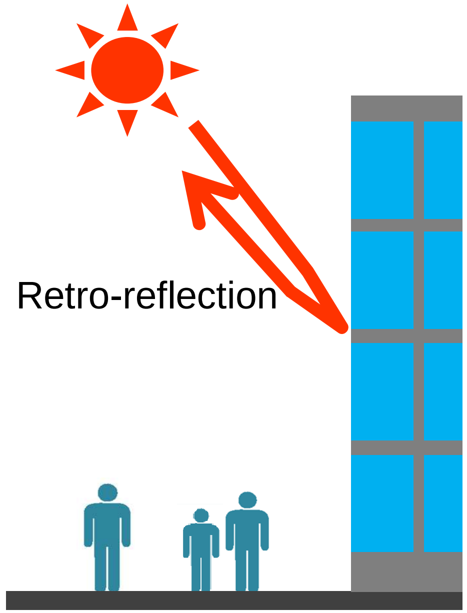

- In order to evaluate effects of installing the heat ray retro-reflective film quantitatively, …

  ⇩

Necessity in application of radiant computational method to the evaluation.

Background of this study (3)

- Existing computational methods for analyzing the radiant environment in outdoor spaces (e.g., Yoshida et al. 2006) enable us to …

  ⇒ estimate the three-dimensional distributions of incident short- and long-wave radiation on pedestrians.

  ⇒ evaluate the radiant thermal comfort of pedestrians.

- Most of the existing methods do not allow us to evaluate the effects of a heat ray retro-reflective film for windows on the thermal environment in urban and building spaces.

  [Each surface in the computational domain is assumed to be a perfectly diffuse (or Lambertian) surface.]

Purpose of this study

- In this study, we carried out ...

1) Incorporation of the effects of the directional reflectivity of surfaces into the existing computational method.

1) Evaluation on the effect of a window with a heat ray retro-reflective film on the thermal environment of an outdoor space.

Table of Contents

1.Background and purpose

2. Outline of revised method for radiant computation

3. Outline of analysis

4. Results and discussion

5. Conclusion

2. Outline of revised method for radiant computation

2.1 Existing method for radiant computation

Radiosity, or the total radiation energy flux leaving a surface per unit area and unit time R_i [W]

$$R_i = E_i + \rho_i \sum_{j=1}^{N} F_{ji} R_j \qquad [1]$$

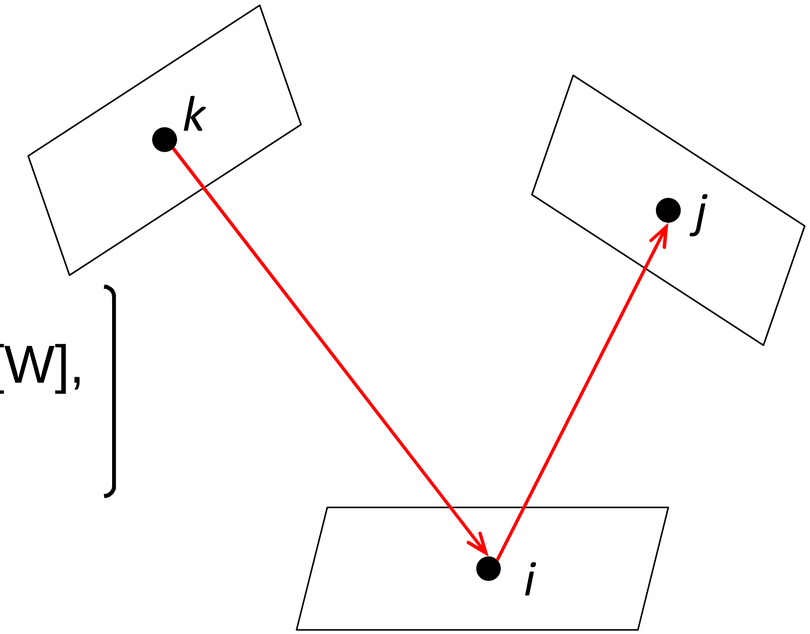

ρ_i is the reflectance of the surface element *i*,
E_i is the radiation emitted at the surface element *i* [W],
F_{ij} is the form factor from *i* to *j*.

The radiosity of surface element *i* intercepted by a surface element *j* per unit of solid angle $R_{i(j)}$ [W/sr]

$$R_{i(j)} = R_i / \pi \qquad [2]$$

2.2 Equations for radiant computation considering directional reflection

$R_{i(j)}$: the radiosity per unit solid angle of surface element i intercepted by surface element j [W/sr]

directional refectivity per solid angle [1/sr]

$$R_{i(j)} = E_{i(j)} + \sum_{k=1}^{N} \kappa_{ki} F_{ki} \cdot \rho_{ki(j)} \cdot \pi \cdot R_{k(i)} \qquad [3]$$

κ_{ki} : the correction coefficient of the distribution of the reflected radiosity from surface k to surface i

$$\kappa_{ki} = \rho_{hemi(k,i)} / \sum_{j=1}^{N} F_{ij} \cdot \pi \cdot \rho_{ki(j)} \qquad [4]$$

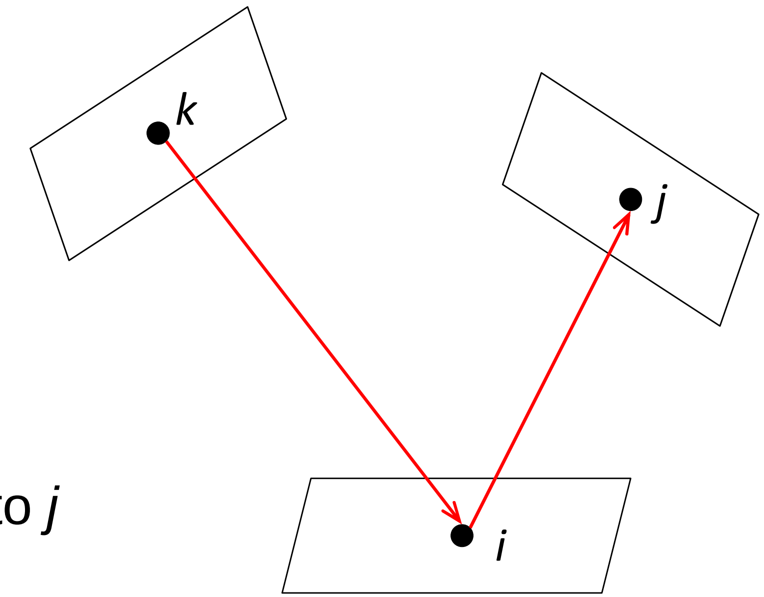

$E_{i(j)}$: the sum of the reflective components of incident, direct, and diffusive solar radiation at surfaces i to j

$$E_{i(j)} = \rho_{(\theta_S,\varphi_S;\, i,j)} E_{Di} + \sum_{k=1}^{N_{sky}} \kappa_{ki} \rho_{ki(j)} A_i F_{ik} I_{SH} \qquad [5]$$

directional refectivity per solid angle

Calculation of directional reflectivity per unit solid angle

Application of the anisotropic body of rotation of the normal distribution function (AND) model

[Makino, T., A. Nakamura, and H. Wakabayashi. 1999. "Directional characteristics of radiation reflection on rough metal surfaces with description of heat transfer parameters." *The Japan society of mechanical engineering*, B, 65, 630: 324-330 (in Japanese with English abstract).]

$$\rho_{(\theta_i;\theta_o;\varphi_o)} = \rho_{D(\theta_i)} + \rho_{s(\theta_i;\theta_o;\varphi_o)}$$

$$\rho_{s(\theta_i;\theta_o;\varphi_o)} cos\theta_o = A \cdot exp(-f^2/2\sigma^2)\cos\{(\pi/2)(f/g)^2\}$$

Directional reflective component

$$f = \sqrt{(p^2 + q^2)}$$

$$g = (kp + \sqrt{f^2 - k^2 q^2})/f$$

$$p = \sin\theta_o \cos(\varphi_o - \varphi_{o(max)}) - k$$

$$q = \sin\theta_o \sin(\varphi_o - \varphi_{o(max)})$$

$$k = \sin\theta_{o(\max)}$$

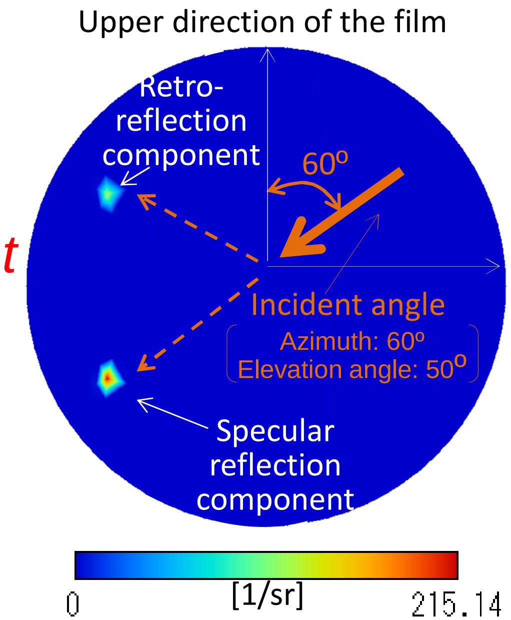

Distributions of reflectance of heat ray retro-reflective film per solid angle on hemisphere centering an intercept point of the incident radiation

Table of Contents

1. Background and purpose

2. Outline of revised method for radiant computation

3. Outline of analysis

4. Results and discussion

5. Conclusion

3. Outline of the analysis

3.1 Study area

Domain : Only one building stands in a domain.

(for evaluating only the effect of a heat ray retro-reflective film on the thermal environment of an outdoor space, clearly.)

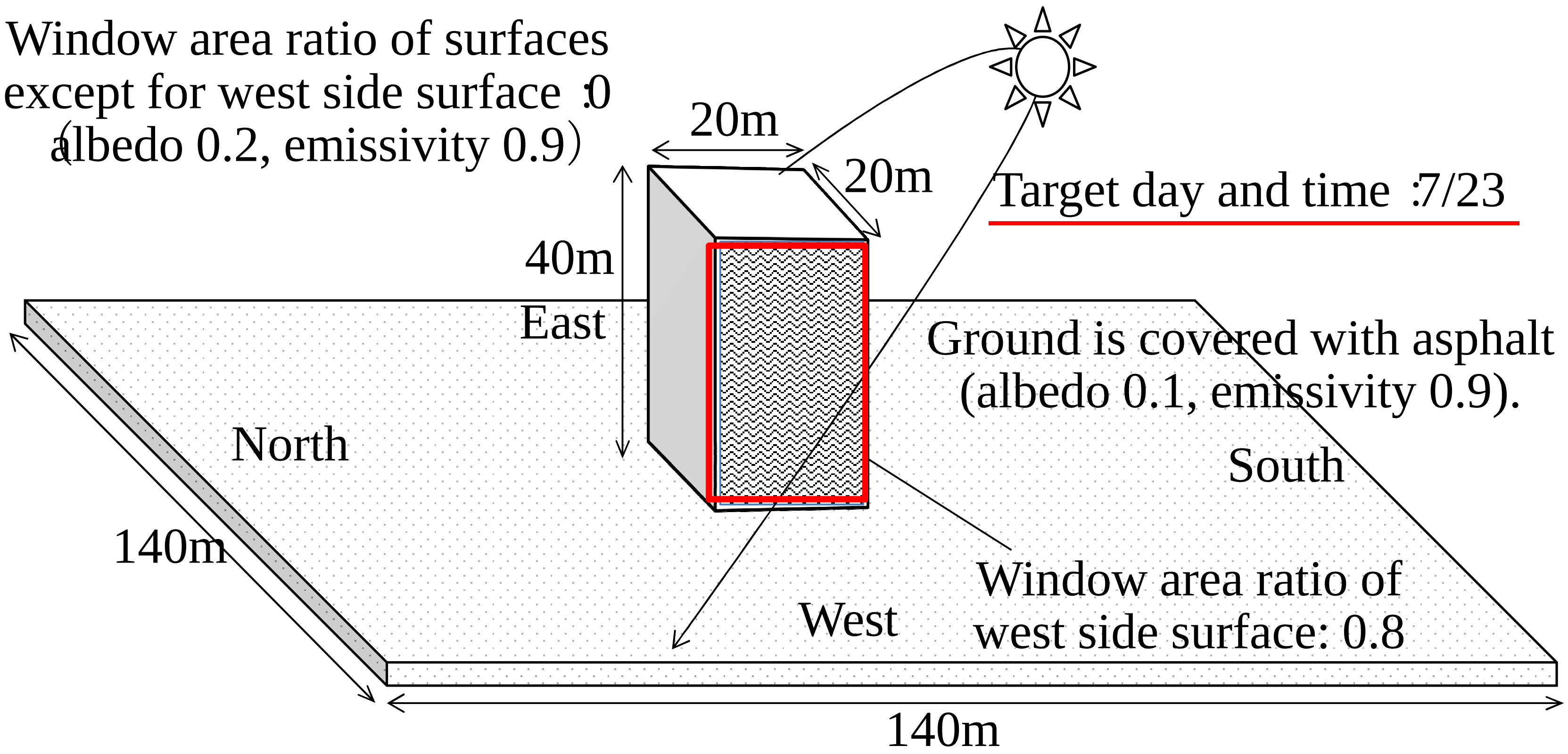

3. Outline of the analysis

3.1 Study area

Domain : Only one building stands in a domain.

(for evaluating only the effect of a heat ray retro-reflective film on the thermal environment of an outdoor space.)

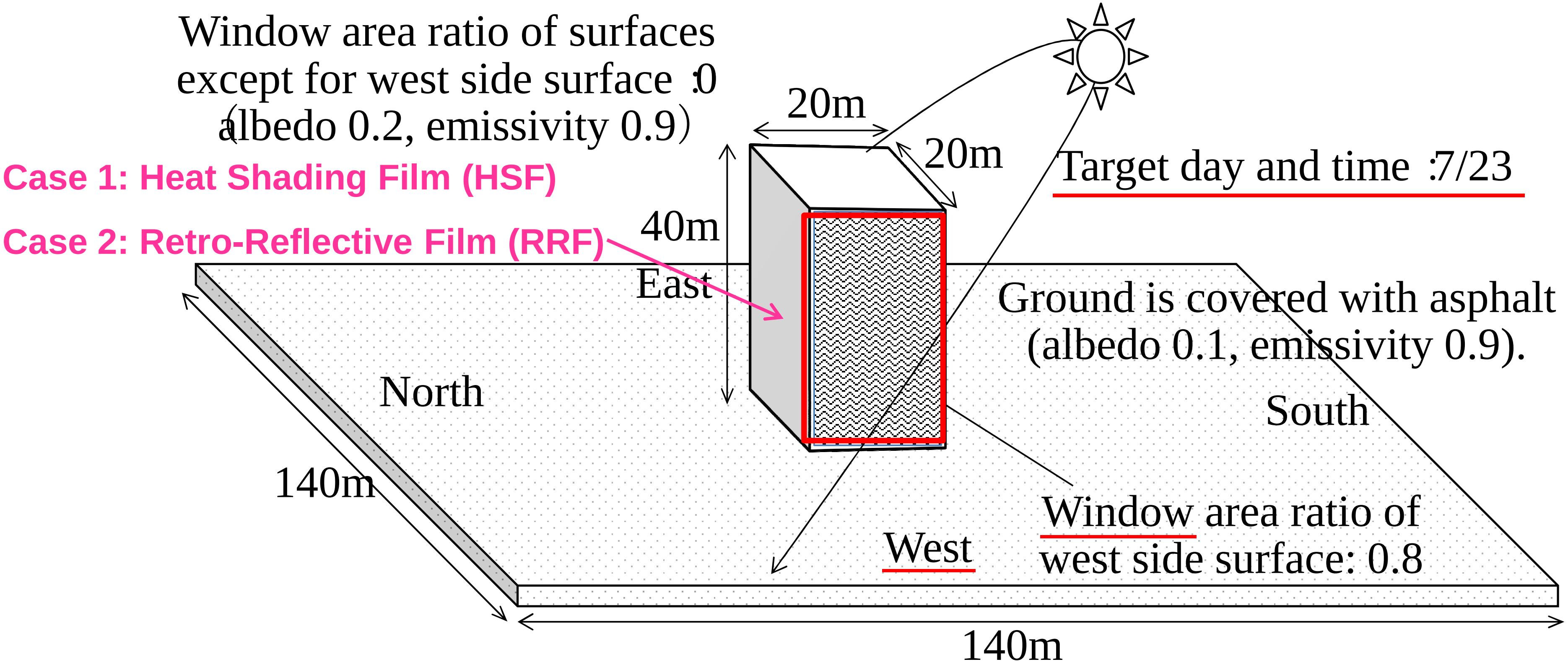

3.2 Meteorological conditions

The target period: 7/22 to 23 in 2010

The time for evaluating the thermal environment on pedestrian space: 14:00 on 7/23.

case	case 1
Target time	14:00 on 23rd July in 2010
Weather	A particular hot summer day
Global solar radiation [W/m^2]	777.8
Sun's altitude [deg]	57.1
Sun's azimuth [deg]	71.1 (nearly WSW)
Air temperature [ºC]	34.9
Relative humidity [%]	49
Wind direction and velocity	SSE, 1.2m/s

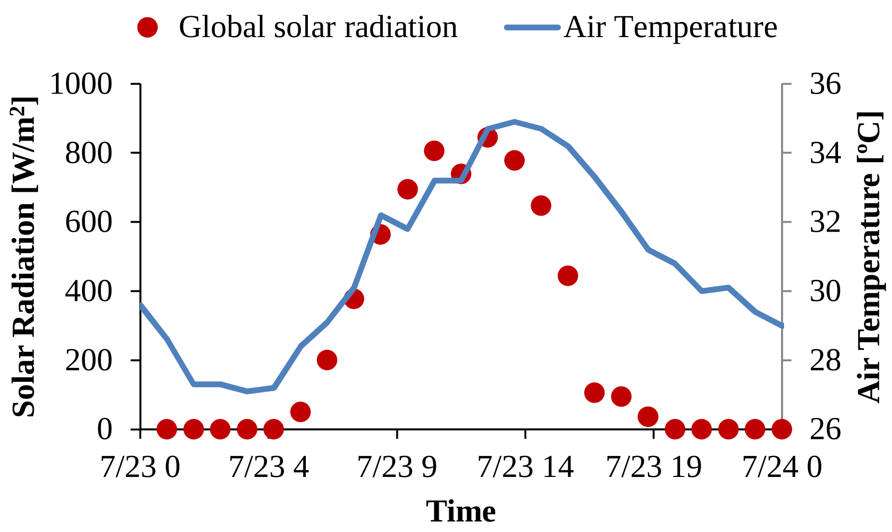

Time variations of global solar radiation and air temperature.

3.3 Computational cases

The following two computational cases were investigated.

Case1: Single-float glass with a heat-shading film (HSF) was used for the western window of the building

Case2: Single-float glass with a heat ray retro-reflective film (RRF) was used for the western window of the building

Table of Contents

1. Background and purpose

2. Outline of revised method for radiant computation

3. Outline of analysis

4. **Results and discussion**

5. Conclusion

4.1 Performance of each window in reflecting solar radiation

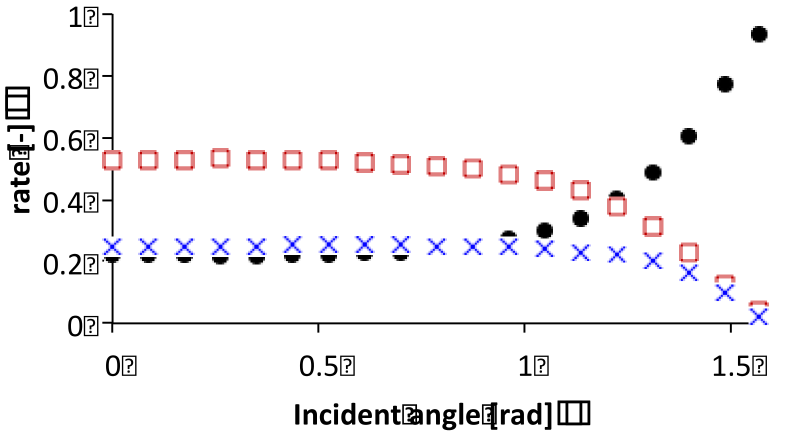

(1) Case1 (HSF, AND model)

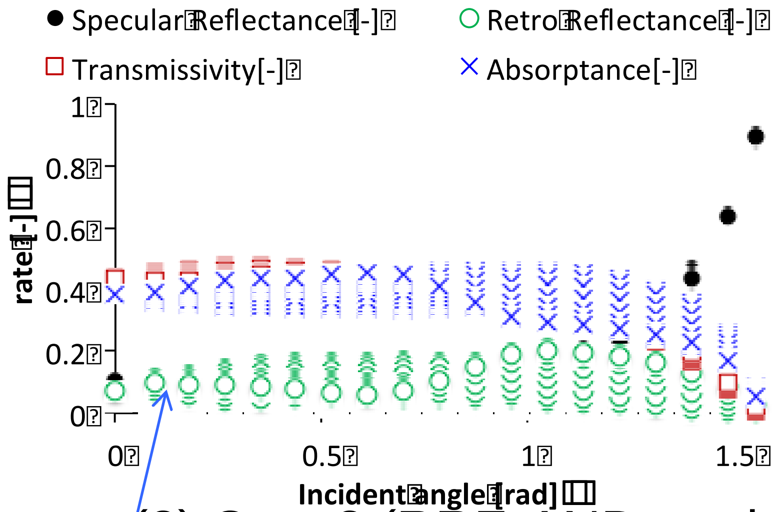

(2) Case2 (RRF, AND model)

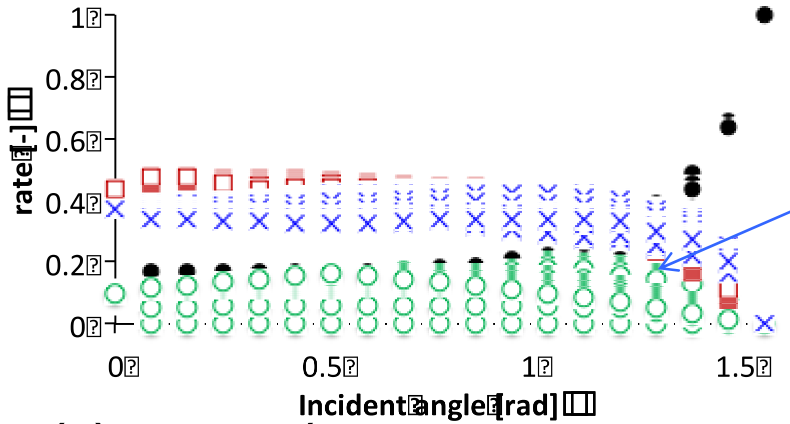

(3) Case2 (RRF, Measurement data)

There is a relatively wide variation.

The incident azimuth and incident elevation angle both affect the radiant properties of the window with the heat ray retro-reflective film.

Distributions of absorptance, reflectance, transmissivity on each incident elevation angle to window

Time variations of total, retro, and specular reflectivity of the retro-reflective window facing the western direction on July 23rd.

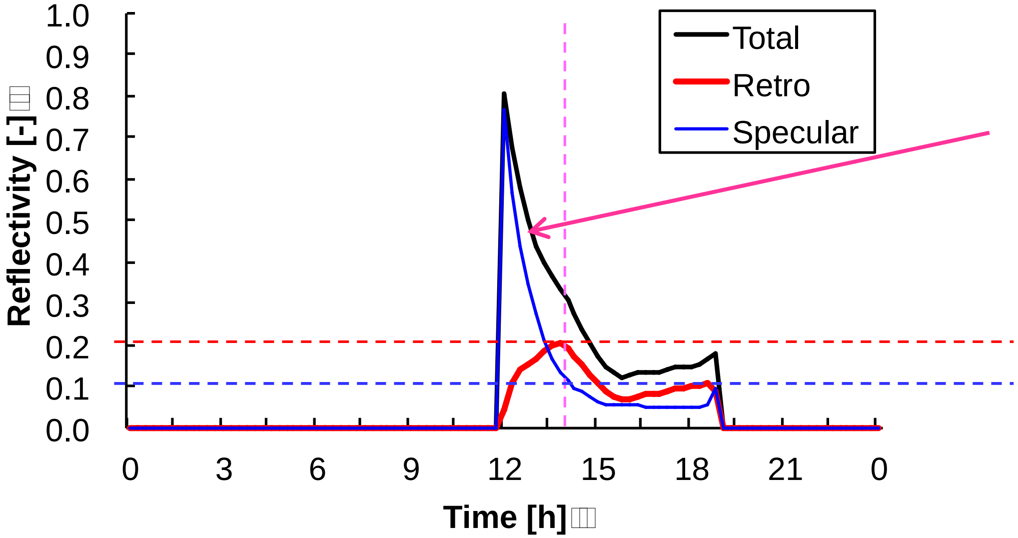

Values decrease dramatically with incident angles of solar radiation.

The value of the retro-reflectivity is approximately twice as much as that of the specular reflectivity at 14:00.

Target time was determined.

(We can see large difference between both cases.)

Investigation on effects of installed windows on specular and retro reflectivity

These values correspond well to the values extracted from model data.

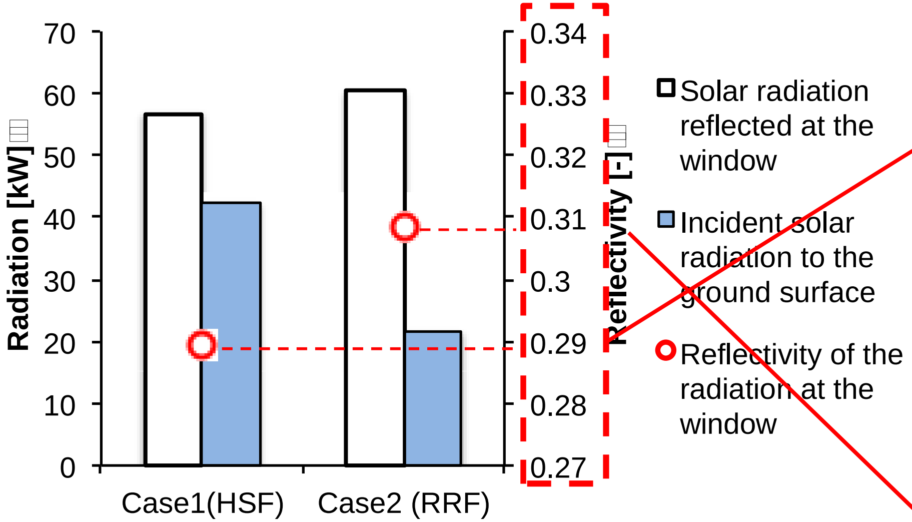

Solar radiant reflectivity on window.

$$\frac{\text{Retro + Specular reflected radiation}}{\text{Directional incident radiation from the sun and the surroundings}}$$

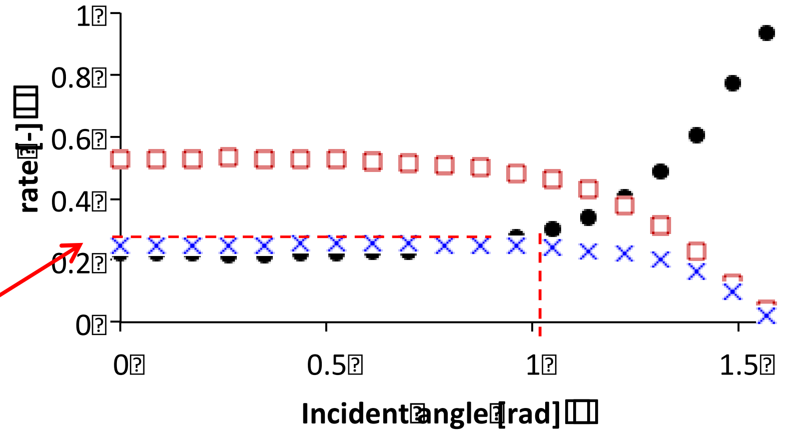

(1) Case1 (HSF)

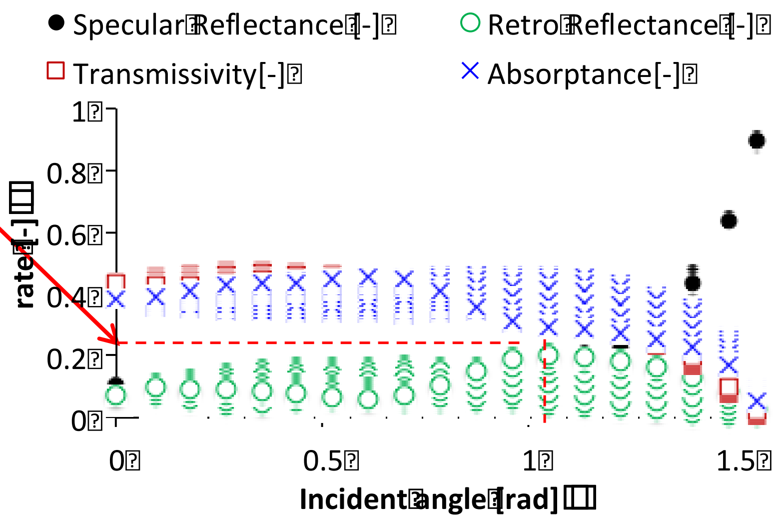

(2) Case2 (RRF)

Relationship between the solar radiation reflected at the western window of the building and the incident radiation to the ground surface near the west side of the building after being reflected at the window

Reflected radiation returning to the sky (Case1: 33%, Case2: 67%)

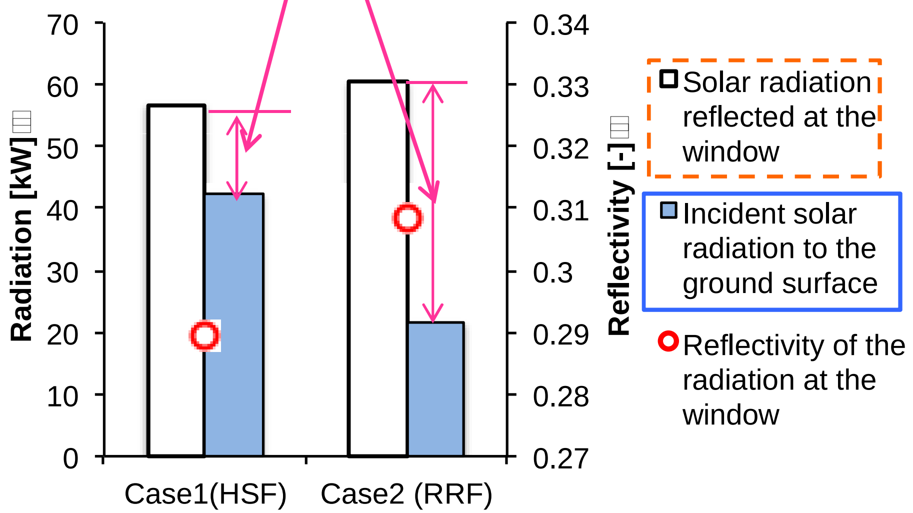

The window in Case2 returns large amount of solar radiation to the sky than Case1.

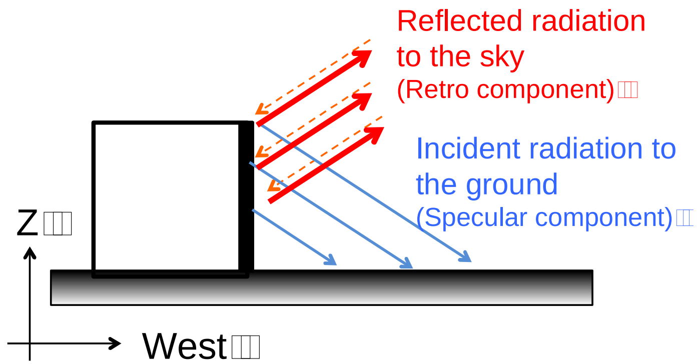

Heat budget between window and ground surface.

Distributions of absorbed solar radiation at the ground surface

The values near the window are considerably larger than those near the surrounding ground surfaces (Effects of specular reflection).

The reduction is caused by the use of the heat ray retro-reflective film (Effects of retro reflection).

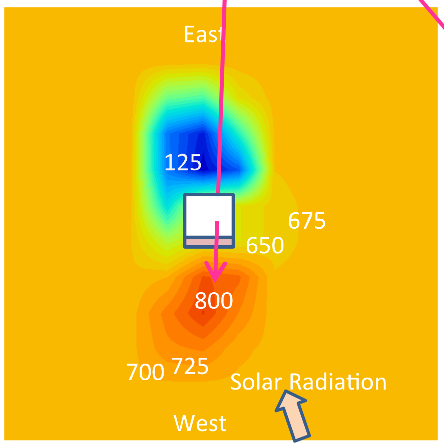

Case 1(HSF)

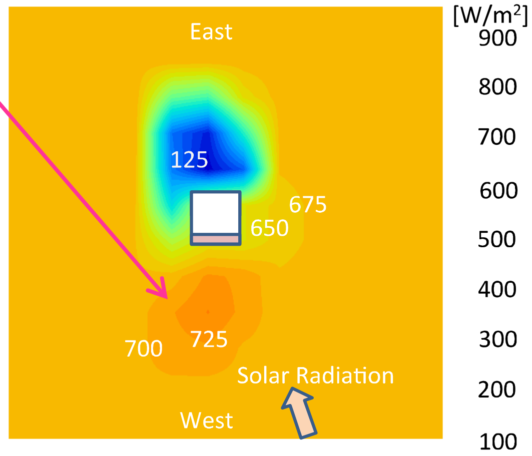

Case 2 (RRF)

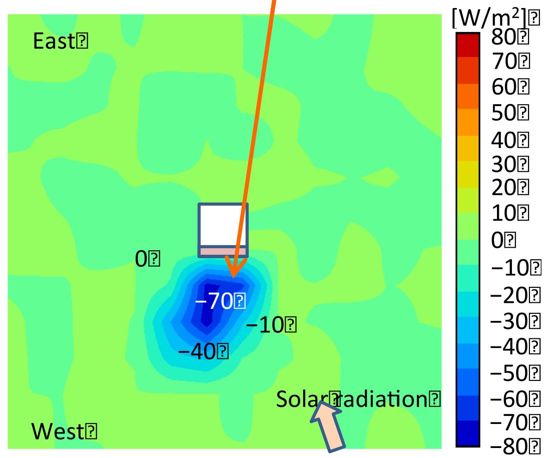

Case2 - Case1

Distributions of absorbed solar radiation and difference between Case2 (Retro- Reflective Film) and Case 1 (Heat-Shading Film) at 14:00 on July 23rd.

4.3 Distributions of ground surface temperature

The trends of the distributions and that of the difference are similar to those for the absorbed solar radiation on the ground surface, shown in previous slide.

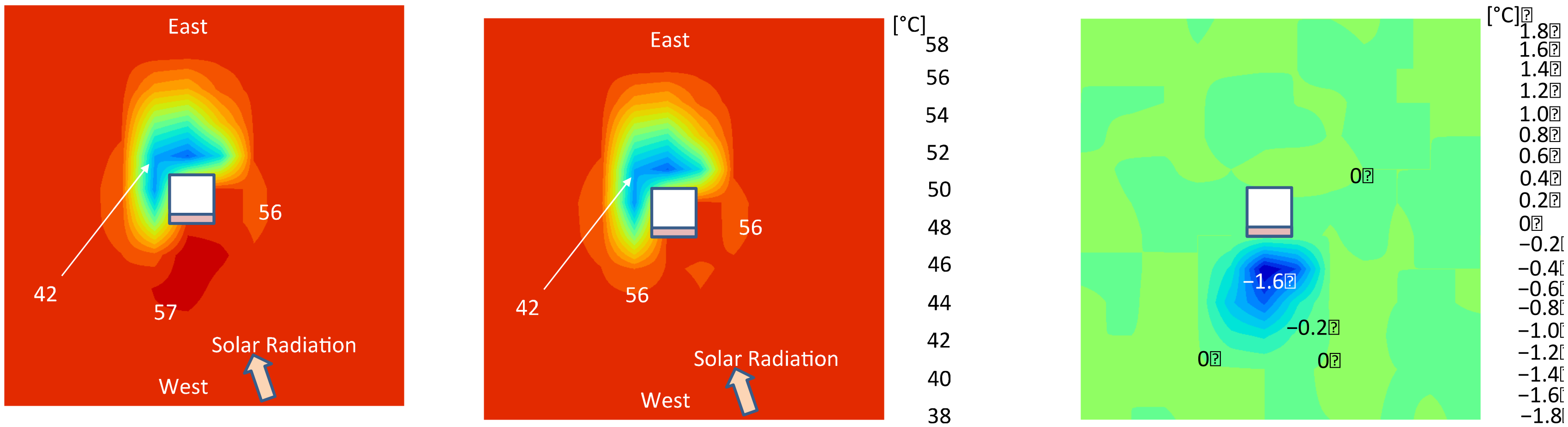

Case 1(HSF) Case 2 (RRF) Case2 - Case1

Distributions of ground surface temperature and difference between Case2 (Retro- Reflective Film) and Case 1 (Heat-Shading Film) at 14:00 on July 23rd.

4.3 Investigation of radiant thermal environment for a pedestrian

We calculated 24 incident solar radiation or MRT values,
where the pedestrian orientation differed by 15° between each value.

Azimuth = 0 (South)

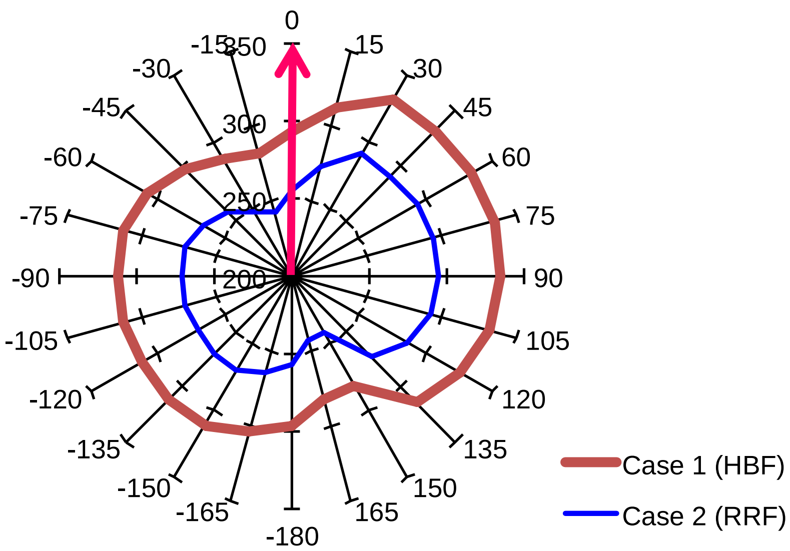

(1) Incident solar radiation

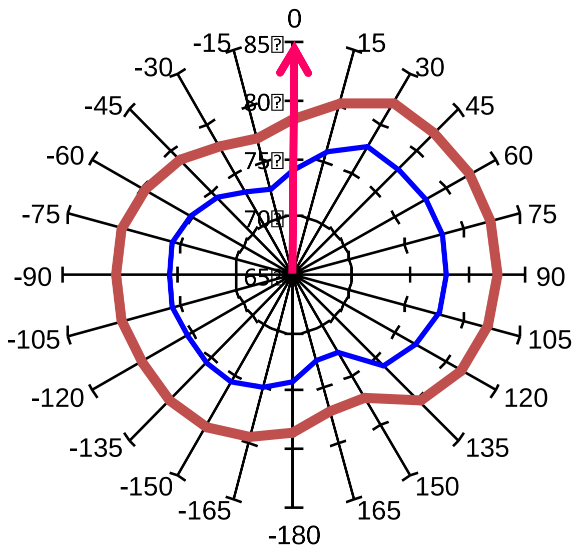

(2)MRT

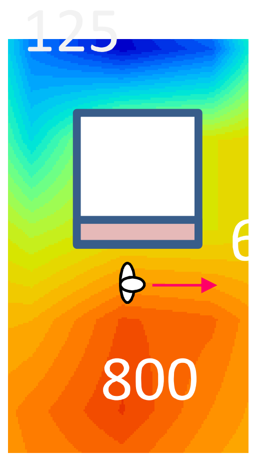

Azimuthal distributions of solar radiation and MRT for the entire body of a pedestrian facing each direction at 14:00 on July 23rd.

4.3 Investigation of radiant thermal environment for a pedestrian

We calculated 24 incident solar radiation or MRT values,
where the pedestrian orientation differed by 15° between each value.

Azimuth = 45 (SW)

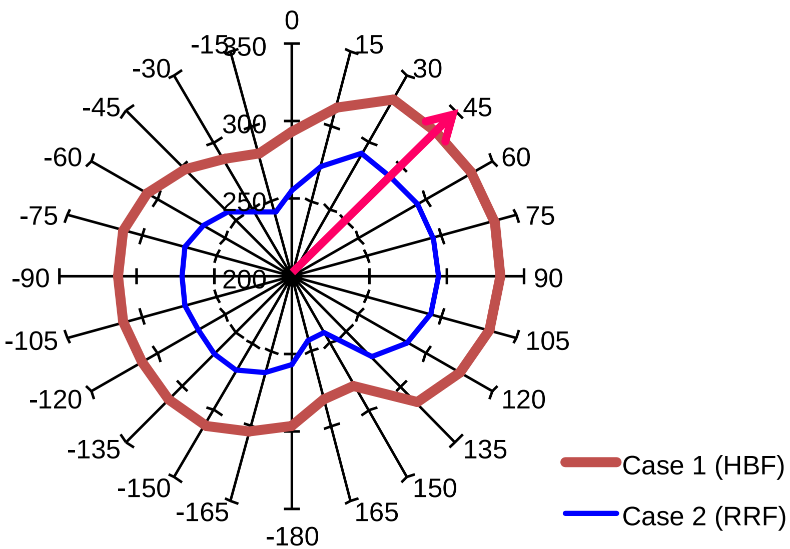

(1) Incident solar radiation

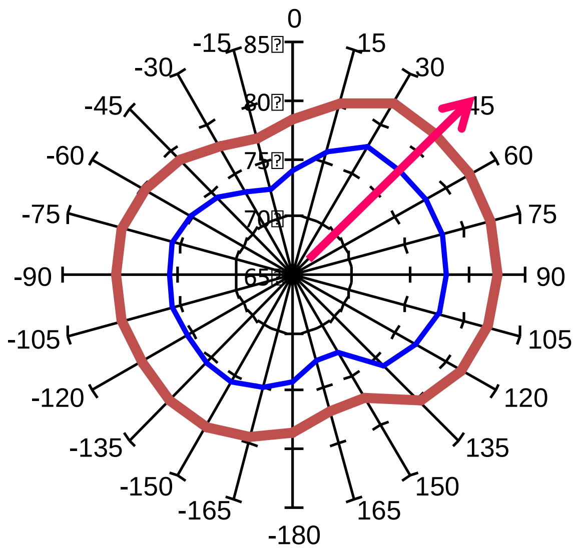

(2)MRT

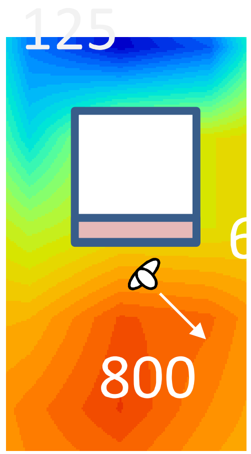

Azimuthal distributions of solar radiation and MRT for the entire body of a pedestrian facing each direction at 14:00 on July 23rd.

4.3 Investigation of radiant thermal environment for a pedestrian

We calculated 24 incident solar radiation or MRT values,
where the pedestrian orientation differed by 15° between each value.

Azimuth = 90 (West)

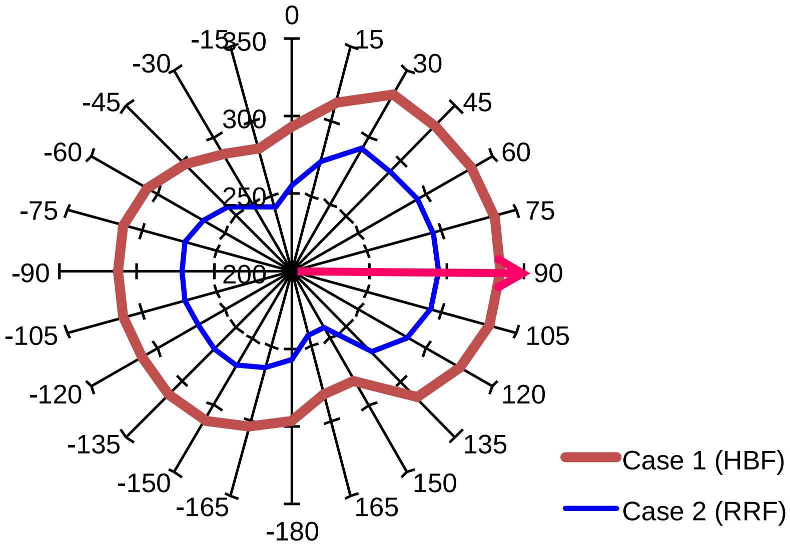

(1) Incident solar radiation

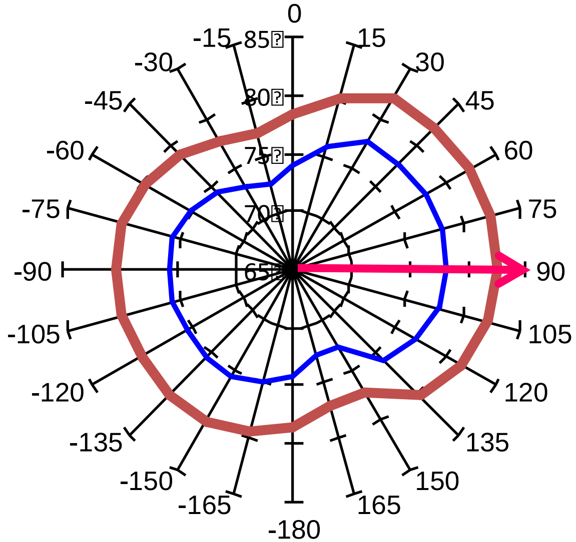

(2)MRT

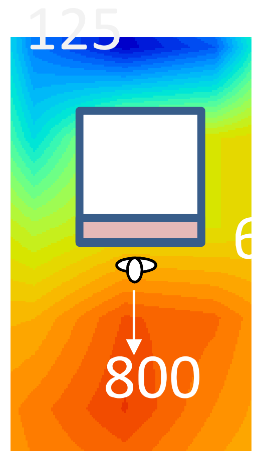

Azimuthal distributions of solar radiation and MRT for the entire body of a pedestrian facing each direction at 14:00 on July 23rd.

4.3 Investigation of radiant thermal environment for a pedestrian

We calculated 24 incident solar radiation or MRT values,
where the pedestrian orientation differed by 15° between each value.

Azimuth = 135 (NW)

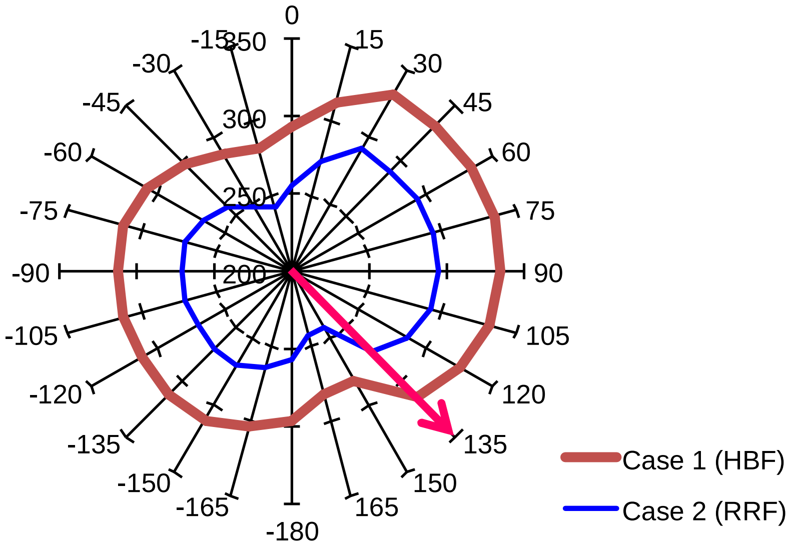

(1) Incident solar radiation

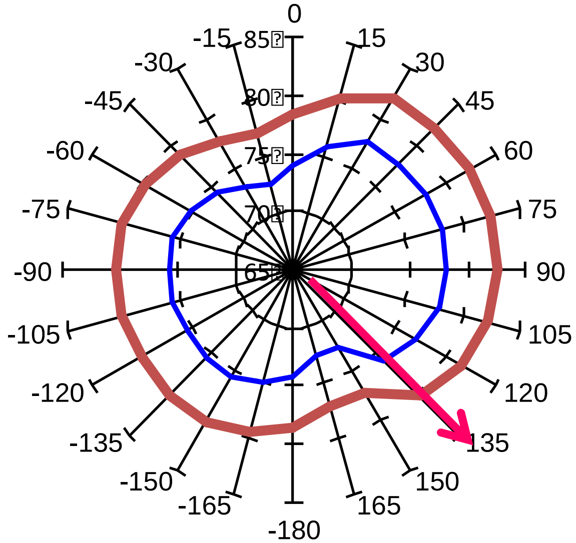

(2)MRT

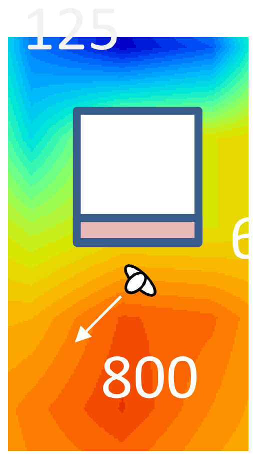

Azimuthal distributions of solar radiation and MRT for the entire body of a pedestrian facing each direction at 14:00 on July 23rd.

4.3 Investigation of radiant thermal environment for a pedestrian

We calculated 24 incident solar radiation or MRT values,
where the pedestrian orientation differed by 15° between each value.

Azimuth = 180 (North)

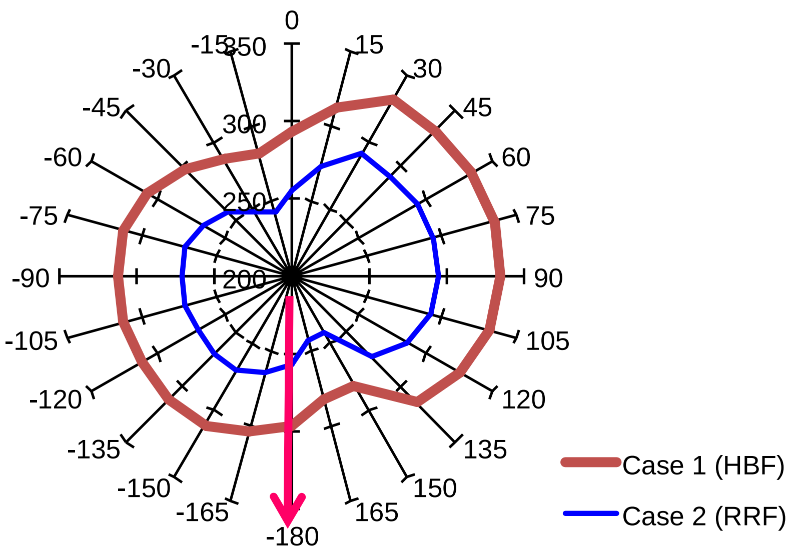

(1) Incident solar radiation

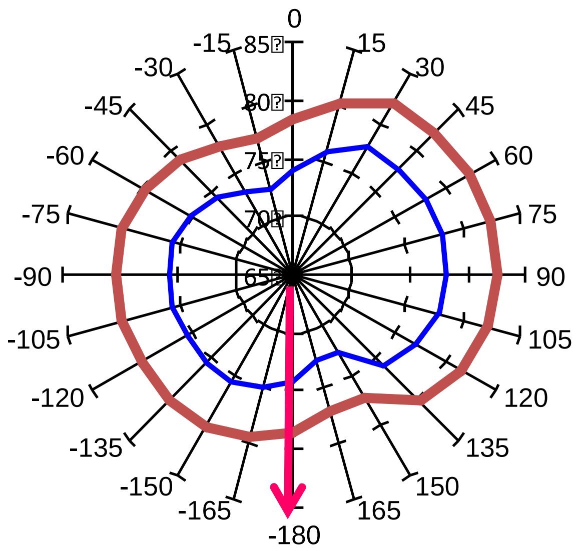

(2)MRT

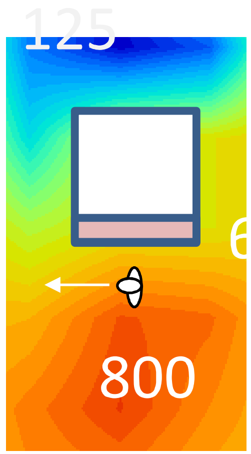

Azimuthal distributions of solar radiation and MRT for the entire body of a pedestrian facing each direction at 14:00 on July 23rd.

4.3 Investigation of radiant thermal environment for a pedestrian

We calculated 24 incident solar radiation or MRT values,
where the pedestrian orientation differed by 15° between each value.

Azimuth = -135 (NE)

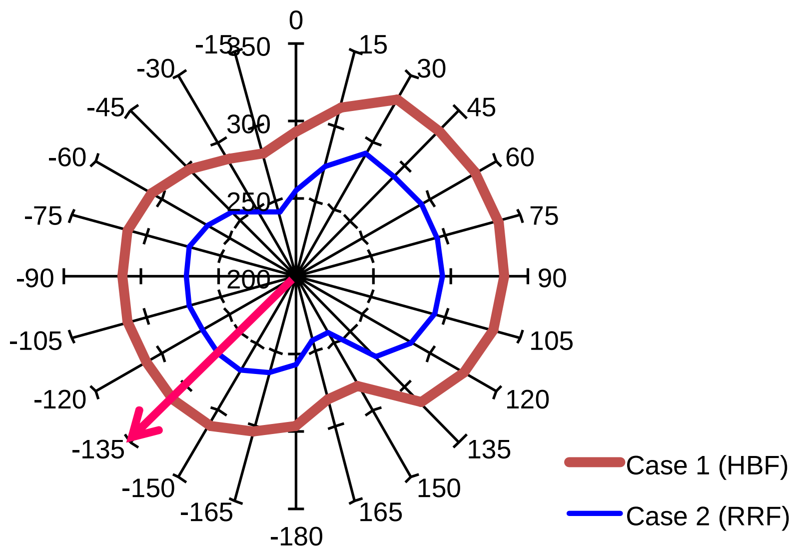

(1) Incident solar radiation

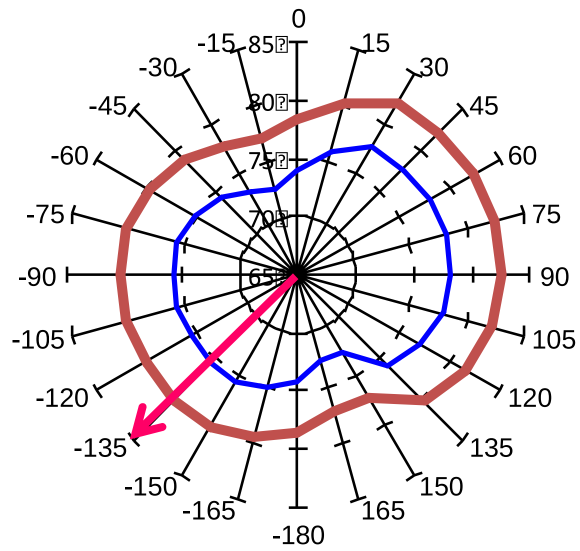

(2)MRT

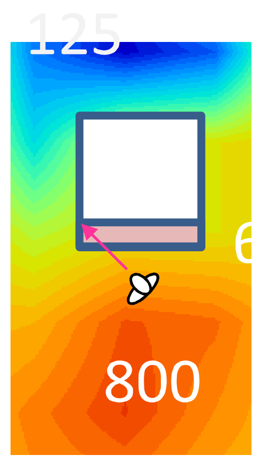

Azimuthal distributions of solar radiation and MRT for the entire body of a pedestrian facing each direction at 14:00 on July 23rd.

4.3 Investigation of radiant thermal environment for a pedestrian

We calculated 24 incident solar radiation or MRT values,
where the pedestrian orientation differed by 15° between each value.

Azimuth = -90 (East)

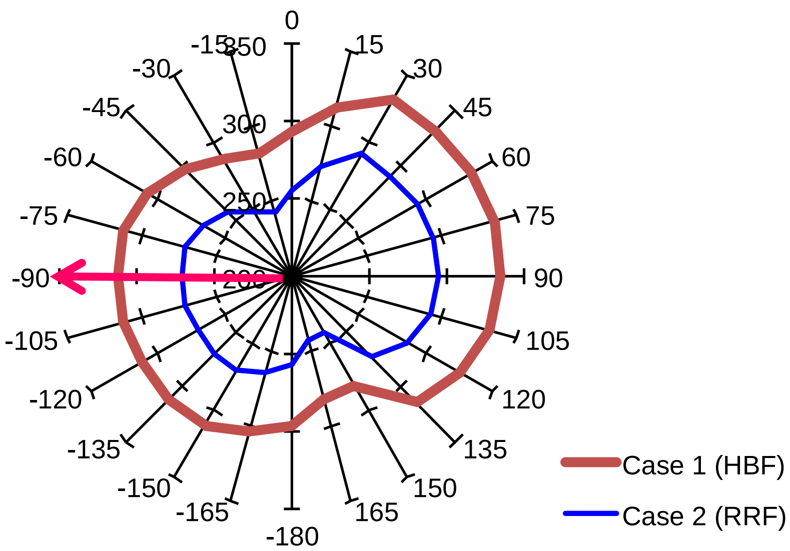

(1) Incident solar radiation

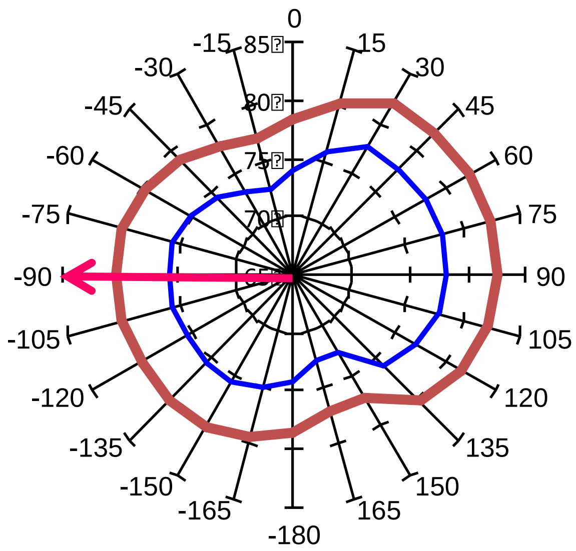

(2)MRT

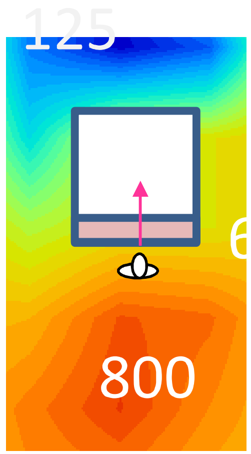

Azimuthal distributions of solar radiation and MRT for the entire body of a pedestrian facing each direction at 14:00 on July 23rd.

4.3 Investigation of radiant thermal environment for a pedestrian

We calculated 24 incident solar radiation or MRT values,
where the pedestrian orientation differed by 15° between each value.

Azimuth = -45 (SE)

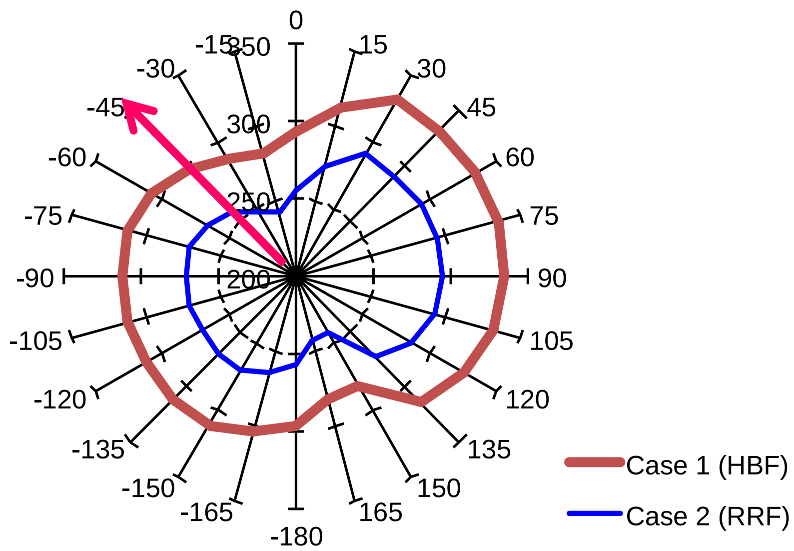

(1) Incident solar radiation

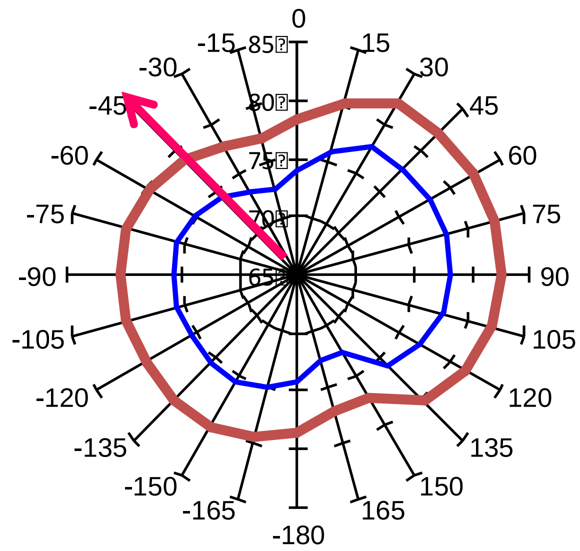

(2)MRT

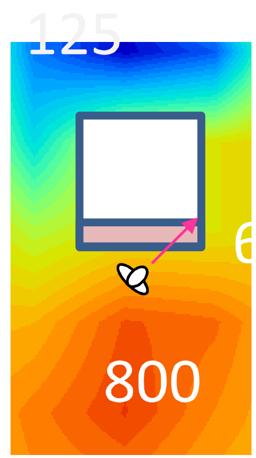

Azimuthal distributions of solar radiation and MRT for the entire body of a pedestrian facing each direction at 14:00 on July 23rd.

4.3 Investigation of radiant thermal environment for a pedestrian

We calculated 24 incident solar radiation or MRT values,
where the pedestrian orientation differed by 15° between each value.

Azimuth = 0 (South)

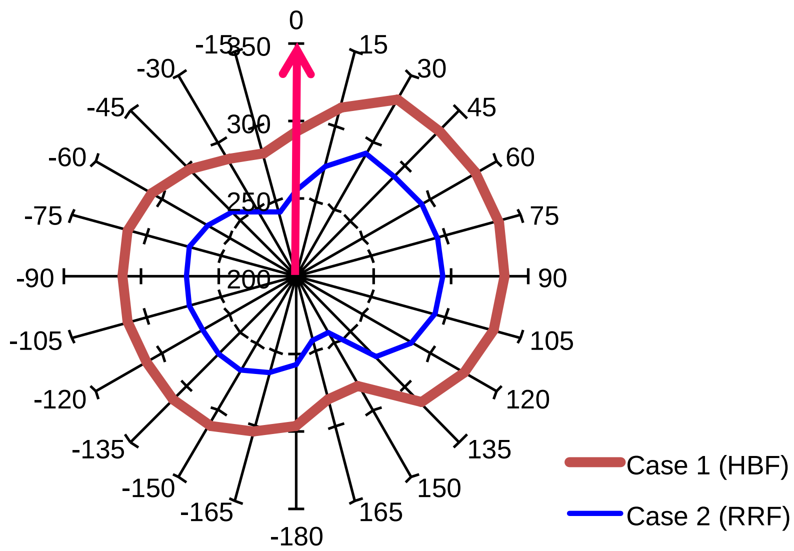

(1) Incident solar radiation

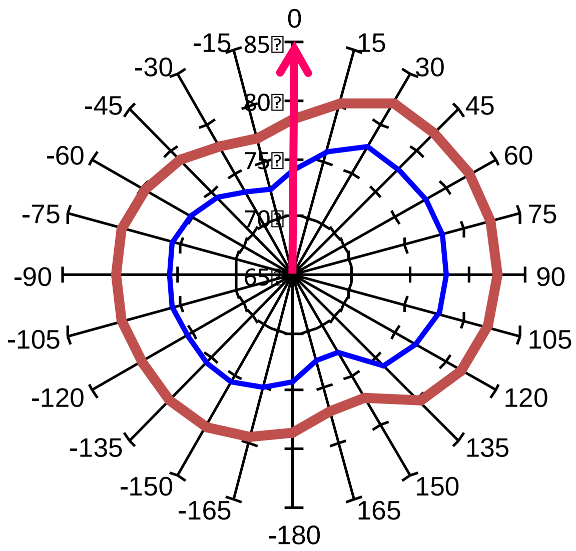

(2)MRT

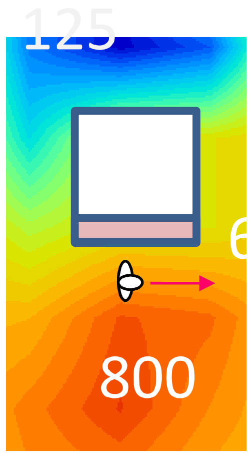

Azimuthal distributions of solar radiation and MRT for the entire body of a pedestrian facing each direction at 14:00 on July 23rd.

The method for analyzing **inhomogeneous radiation** in outdoor space (Yoshida et al. at ICUC7)

(1) Set **virtual spheres** centering around a human body

(2) Distributions of solar and longwave radiations on **each surface element comprising the spheres**

(3) Distributions of solar and longwave radiations on **each body segment**

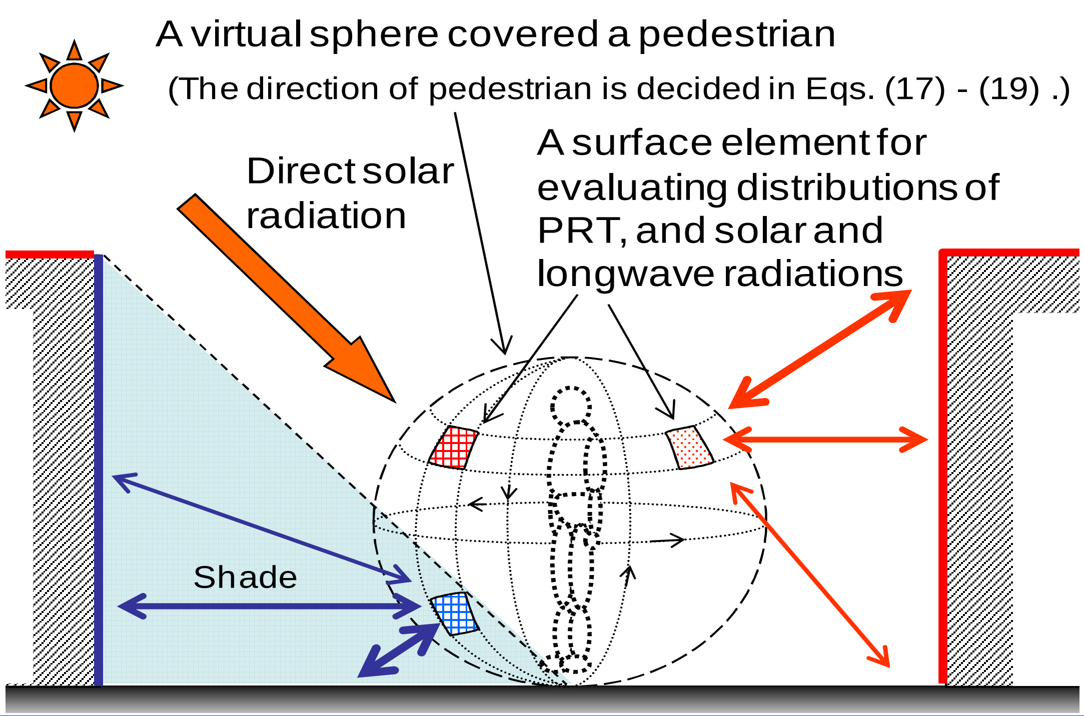

4.3 Investigation of radiant thermal environment for a pedestrian

Values from southwest of the azimuth to west were relatively large.

Solar radiation irradiating from the front orientation side is slightly larger than that from the back side direction.

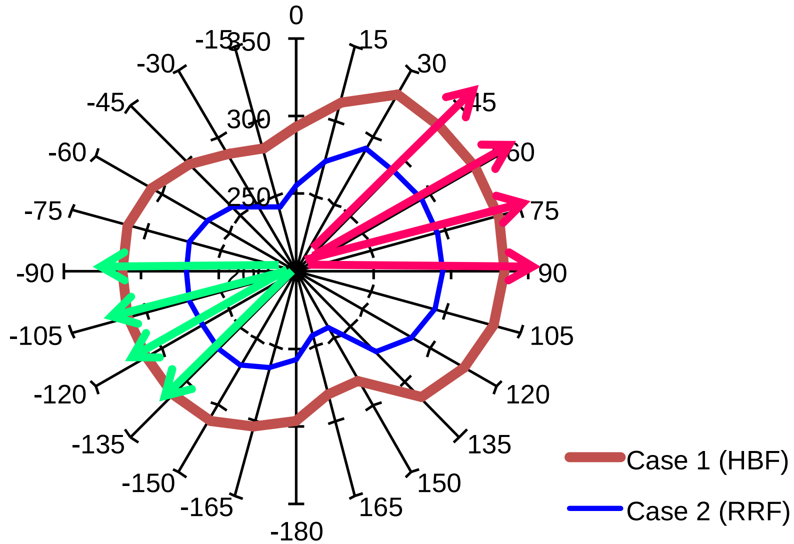

(1) Incident solar radiation

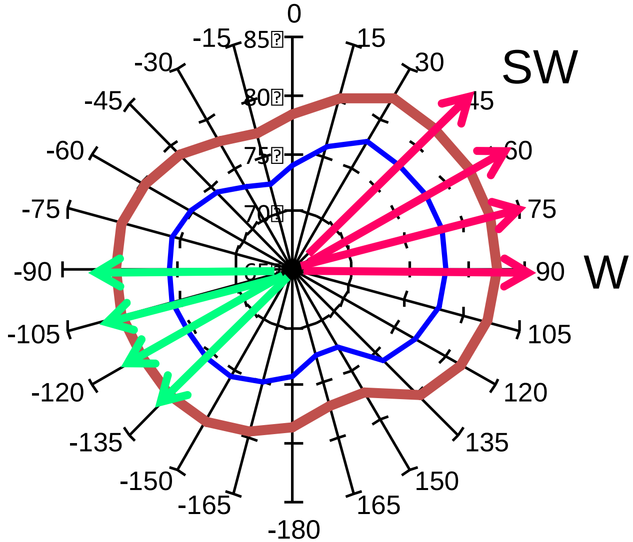

(2)MRT

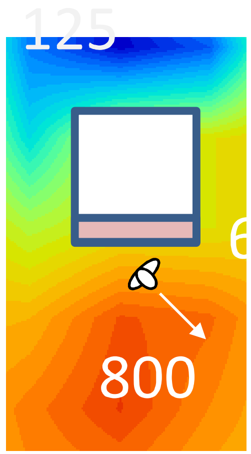

Azimuthal distributions of solar radiation and MRT for the entire body of a pedestrian facing each direction at 14:00 on July 23rd.

4.3 Investigation of radiant thermal environment for a pedestrian

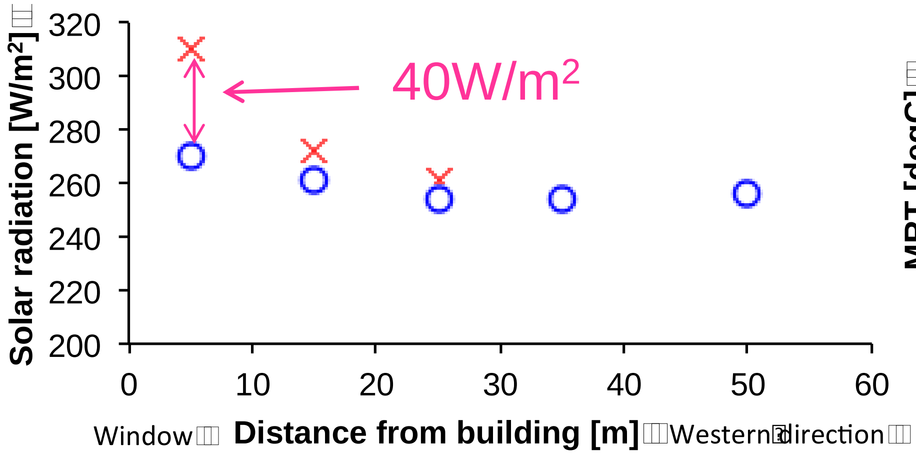

(1) Incident solar radiation

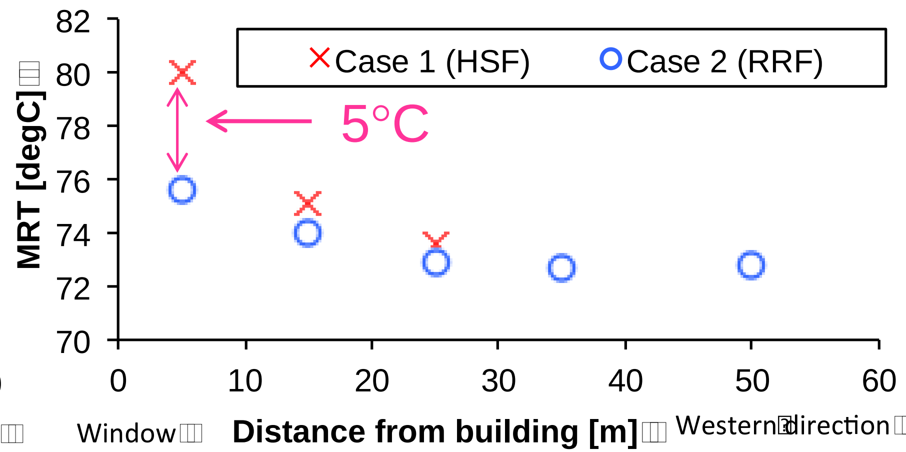

(2)MRT

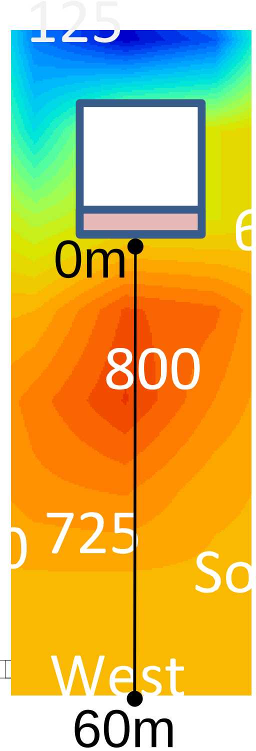

Distributions of incident solar radiation and MRT for the entire body of a pedestrian from near the window of building to western direction.

The values in the figure are averages of the 24 incident solar radiation or MRT values shown in the previous figure.

4.3 Investigation of radiant thermal environment for a pedestrian

We calculated 24 incident solar radiation or MRT values, where the pedestrian orientation differed by 15° between each value.

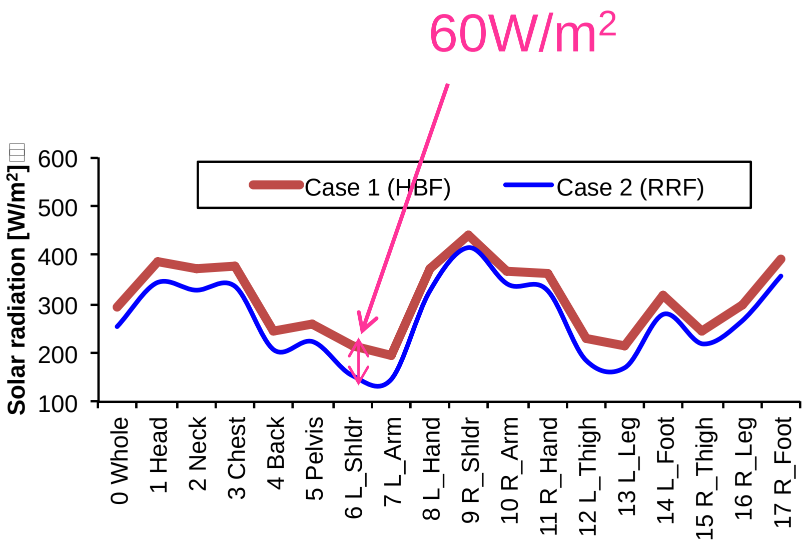

(1) Orientation of a pedestrian is 0° (South)

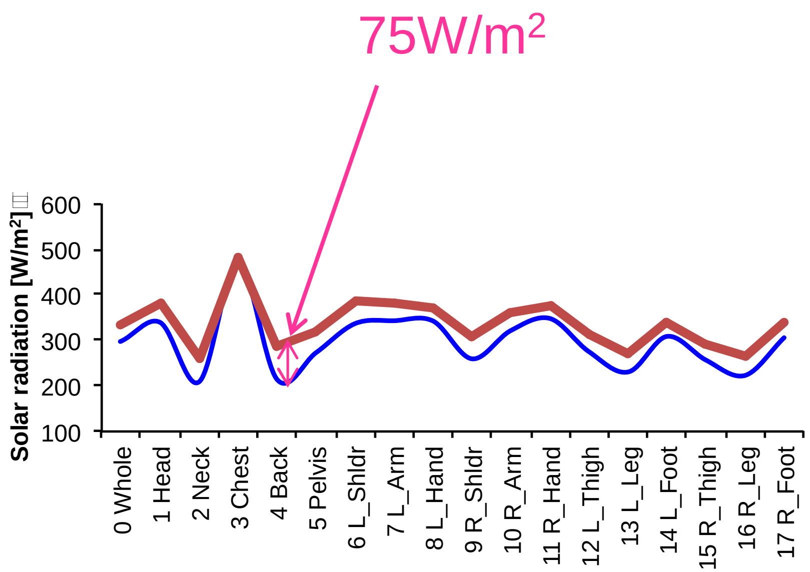

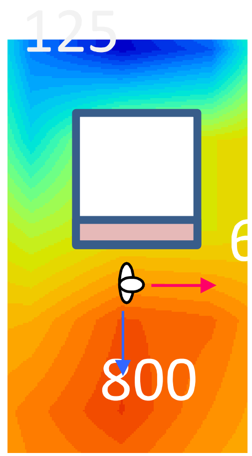

(2) Orientation of a pedestrian is 90° (West)

Distributions of incident solar radiation on each body segment for the pedestrian at 14:00 on July 23rd.

4.3 Investigation of radiant thermal environment for a pedestrian

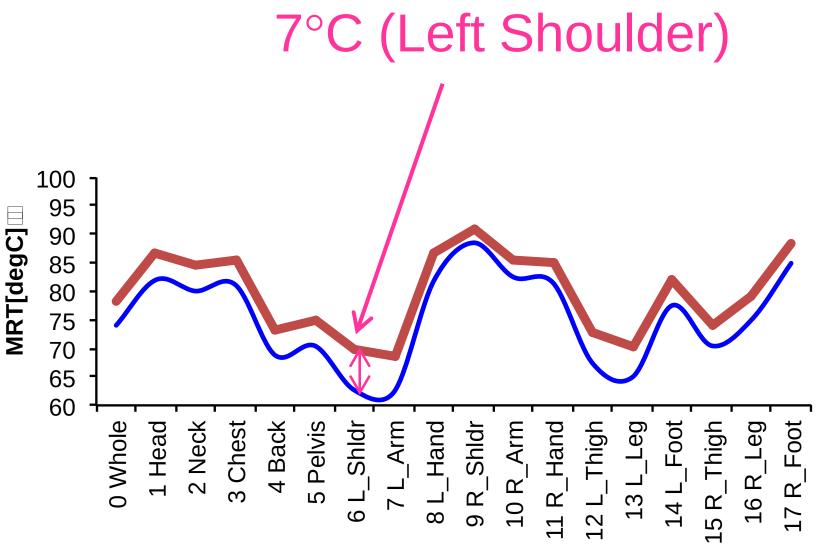

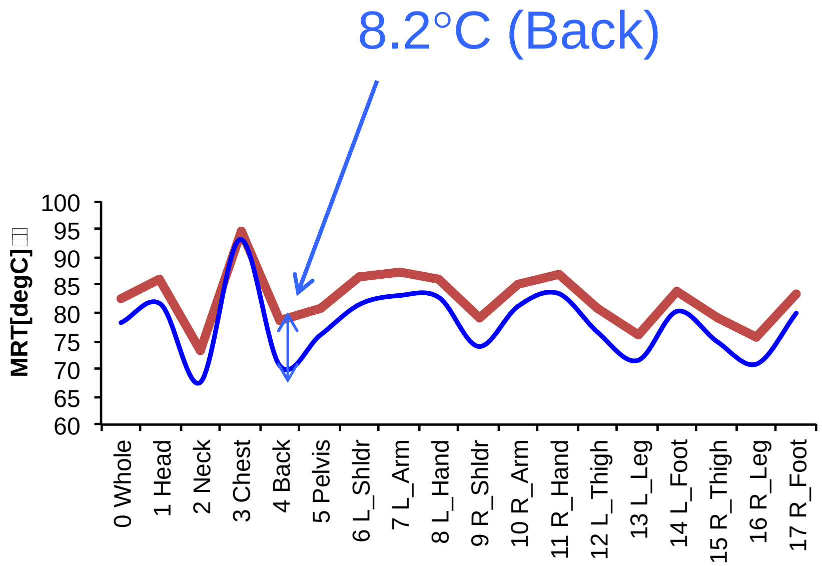

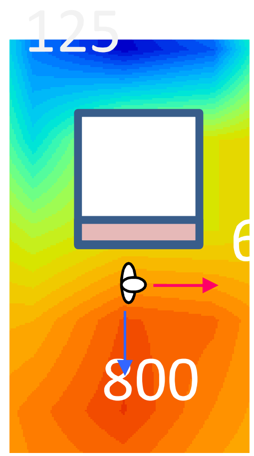

(1) Orientation of a pedestrian is 0° (South)

(2) Orientation of a pedestrian is 90° (West)

Distributions of MRT on each body segment for the pedestrian at 14:00 on July 23rd.

Table of Contents

1. Background and purpose

2. Outline of revised method for radiant computation

3. Outline of analysis

4. Results and discussion

5. Conclusion

4. Conclusions

[1] Proposal of a computational method for radiant thermal environment in outdoor space with consideration of directional reflection.

[2] Application of the proposed method to evaluating the radiant environment around a single building for two different glazing types of window surface.

(From the analysis, it has been found that ...)

(1) The amount of radiation reflected to the sky using a window with heat ray retro-reflective film was equivalent to twice the radiation reflected using a window with heat shading film,

(2) The MRT around the retro-reflective window was lower by up to 5°C than that around the heat-shading window.

[3] Future study:

Application of this method to analyzing thermal environment in a real town block for evaluating the effects of the heat ray retro-reflective film.

Thank you for your kind attention!

Shinji Yoshida　(University of Fukui)

y-shinji@u-fukui.ac.jp